region, it is difficult to estimate the relative effectiveness of Joulean and annihilation dissipation as a trigger mechanism because of the completely different spatial distributions.

ACKNOWLEDGMENTS

The experimental work to which these computations relate was done at the Bell Telephone Laboratories, Inc., Murray Hill, New Jersey, during a recent sabbatical. The author gratefully acknowledges his indebtedness to Dr. Y. B. Kim and his group there. For the impetus to undertake these detailed computations the author is indebted to Professor dr. M. J. Steenland, Technische Hogeschool te Eindhoven, and, for many stimulating discussions, to Dr. M. R. MacPhail, Rice University.

PHYSICAL REVIEW VOLUME 154, NUMBER 2 10 FEBRUARY 1967

Superconducting- and Normal-State Thermal Conductivity of Impure Tin*

G. J. Pearson,† C. W. Ulbrich,‡ J. E. Gueths,‡ M. A. Mitchell, and C. A. Reynolds
Physics Department and Institute of Materials Science, University of Connecticut, Storrs, Connecticut
(Received 12 August 1965; revised manuscript received 20 June 1966)

Low-temperature measurements of the normal- and superconducting-state thermal conductivities were made on ten tin specimens, one of which was pure (99.996%) and nine of which were lightly doped (up to 1 at.%) with mercury, lead, or bismuth. The ratios K^s/K^n of the superconducting- to normal-state thermal conductivity are used to analyze the data. The normal-state thermal conductivity is assumed to consist of a fractionally small lattice component $K_g{}^n$ consistent with the "universal-curve" formalism of Lindenfeld and Pennebaker, added to a much larger electronic component of the Wiedemann-Franz type. The superconducting lattice thermal conductivity $K_g{}^s$ is assumed to be simply related to $K_g{}^n$ in a manner roughly independent of impurity concentration. Proceeding in this manner, it is shown that the variation of K^s/K^n with changing electronic mean free path is consistent with a normal-state lattice conductivity having a temperature dependence similar to that observed by other investigators on other alloy systems. Furthermore, if one *quantitatively* adopts the "universal-curve" formalism, it is seen that the analysis yields a temperature-dependent ratio of lattice conductivities, $K_g{}^s/K_g{}^n$, which is consistent with the theory of Bardeen, Rickayzen, and Tewordt. The thermal conductivities of the pure and the three lowest impurity samples are mostly electronic, and thus it is possible to compare their K^s/K^n ratio with the theoretical $K_e{}^s/K_e{}^n$ ratio of Kadanoff and Martin, calculated for an isotropic gap. The pure-sample data fit the theory with a value of $3.3k_BT_c$ for the superconducting energy gap. However, a value of $3.9k_BT_c$ is found for the gap for the three impure samples.

I. INTRODUCTION

DESCRIBED herein are the results of measurements taken at liquid-helium temperatures on each of one pure and nine impure samples of tin. Of primary interest is the thermal conductivity in the normal and superconducting states. Electrical resistivity and superconducting transition temperature determinations were also made to aid in the reduction and interpretation of the data.

We express the normal- and superconducting-state thermal conductivities as the sum of two terms, one electronic (e) and one lattice (g), viz:

$$\text{(normal state)} \qquad K^n=K_e{}^n+K_g{}^n, \tag{1}$$

$$\text{(superconducting state)} \qquad K^s=K_e{}^s+K_g{}^s. \tag{2}$$

Previous works on tin[1–5] have shown that in the temperature range of 1–4°K:

(a) For relatively pure samples ($\leq$0.01 at. % impurity) the electronic thermal conductivity in the normal and superconducting states is the dominant mechanism. In particular, the normal-state thermal conductivity is adequately described by

$$1/K_e{}^n=\alpha T^2+\beta/T, \tag{3}$$

where αT^2 is the ideal thermal resistivity, due to scattering of electrons by phonons, and β/T is the electron-impurity scattering term. β is approximately ρ_0/L_0, where ρ_0 is the residual electrical resistivity and L_0 is the theoretical Lorenz number.

(b) At about 1 at. % impurity concentration, the β/T term in Eq. (3) has become large and also the lattice conductivity becomes a detectable portion of the total, of the order of several percent at 4°K.

* Supported by U. S. Air Force Office of Scientific Research Grant No. AF-AFOSR-474-64 and Office of Naval Research Contract No. Nonr 2967(00). Part of a thesis submitted by G. J. Pearson to the University of Connecticut in partial fulfillment of the requirements for the Ph.D. degree in Physics.

** Present address: Eastman Kodak, Rochester, New York.
† Present address: Clemson University, Clemson, South Carolina.
‡ Present address: Wisconsin State University, Oshkosh, Wisconsin.

[1] A. M. Guénault, Proc. Roy. Soc. (London) **A262**, 420 (1961).
[2] J. K. Hulm, Proc. Roy. Soc. (London) **A204**, 98 (1950).
[3] M. Garfinkel and P. Lindenfeld, Phys. Rev. **110**, 883 (1958).
[4] S. J. Laredo, Proc. Roy. Soc. (London) **A229**, 473 (1955).
[5] N. V. Zavaritskii, Zh. Eksperim. i Teor. Fiz. **39**, 1571 (1960) [English transl.: Soviet Phys.—JETP **12**, 1093 (1961)].

(c) Between the two extremes the Wiedemann-Franz law is closely obeyed ($K^n \approx L_0 T/\rho_0$), and it is difficult to separate out the contribution of the lattice.

Zimmerman[6] explained the lattice-conduction contribution in his high-resistivity silver-antimony alloys in terms of Pippard's theory of ultrasonic attenuation.[7] Lindenfeld and Pennebaker[8] extended this model to explain the lattice conductivity of their copper alloys and pointed out that this could be expressed as a universal curve to which the normal-state lattice conductivity of any metal could be compared when properly scaled. More recent data on indium[9] and silver[10] alloys have supported these concepts.

By experimental testing[1,5,11–13] two theoretical calculations based on the BCS model of superconductivity[14] have been shown to be at least qualitatively correct. They are: (1) the calculations of Kadanoff and Martin[15] regarding the temperature dependence of the ratio K_e^s/K_e^n, and (2) the calculation of Bardeen, Rickayzen, and Tewordt[16] (BRT) which gives the ratio of lattice conductivities K_g^s/K_g^n as a function of reduced temperature $t=T/T_c$.

It is the goal of this work to investigate the thermal conductivity of tin in the region of impurity concentration where the electronic thermal conductivity is limited mainly by impurity scattering, and the normal-state lattice conductivity is still a very small part of the total conductivity. As we shall see, the small fractional size of K_g^n will make necessary a rather unconventional form of data analysis. The effective anisotropy of the superconducting energy gap, which has been shown to have large effects on quantities like the superconducting transition temperature,[17] is changing rapidly in this impurity region. We will attempt to examine the temperature-dependent ratio K_e^s/K_e^n as a function of impurity, that is, changing electronic mean free path, for any effects which might be caused by this variation in gap anisotropy.

II. EXPERIMENTAL DETAILS

The samples were prepared by vacuum-melting appropriate amounts of Johnson-Matthey 99.999% pure Sn and the desired impurities and extruding the resulting slugs into long wires approximately 1.5 mm in diameter. Sections to be measured were clipped off and annealed at ~200°C for several days. One pure and nine impure specimens were prepared. Lead, mercury, and bismuth were each used to dope three of the impure specimens to nominal impurity concentrations of 0.01, 0.1, and 1.0 at. %. Electrical resistivity, critical temperature, and thermal conductivity measurements were performed on all of the samples. Upon completion of the measurements, portions of each specimen were analyzed spectroscopically for impurity concentration.

The samples were also examined metallographically at the University of Connecticut Metallurgy Laboratory and were found to possess a polycrystalline structure. The grain size was observed to vary inversely with the impurity concentration, the largest grains occurring in the pure sample where they were found to be one-fifth the length of the specimen. There was no significant decrease in the grain sizes for the samples with approximately 0.1% impurity concentration, but the samples of higher impurity concentration were observed to have grains as small as 0.1 mm.

Temperatures were monitored with $\frac{1}{10}$-W, 47-Ω Allen Bradley carbon resistors which were calibrated during each run against the helium bath using the 1958 He vapor-pressure tables.[18] A suitable mathematical expression relating the resistance to temperature for calibration purposes was found to be

$$\ln R = A + B/T + C \ln T, \tag{4}$$

where A, B, and C are adjustable parameters. The resistances were measured with a specially constructed double Wheatstone bridge having sufficient sensitivity to provide a resolution of ≤ 0.001°K over the temperature range of 1.2–5°K.

Thermal-conductivity measurements were taken in the usual manner—in an evacuated can with the sample suspended by one end from a copper stud in direct thermal contact with the helium bath. Two carbon resistors were cemented onto the sample 6 to 8 cm apart, and a Chromel C wire heater was wound at the bottom end. Teflon-coated copper wire (#36) served as thermometer and heater leads. The resistance thermometers were calibrated against the bath by filling the can with He exchange gas. The can was then evacuated overnight to a pressure of 6×10^{-5} Torr, and on the following day thermal conductivity measurements were made. Below the superconducting transition temperature, normal-state data were taken by applying a longitudinal magnetic field to the sample with a dc solenoid. Heater powers supplied to the sample were such as to maintain temperature differences between thermometers of 0.020–1.0°K.

[6] J. E. Zimmerman, J. Phys. Chem. Solids **11**, 299 (1959).
[7] A. B. Pippard, Phil. Mag. **46**, 1104 (1955); J. Phys. Chem. Solids **3**, 175 (1957).
[8] P. Lindenfeld and W. B. Pennebaker, Phys. Rev. **127**, 1881 (1962).
[9] P. Lindenfeld and H. Rohrer, Phys. Rev. **139**, A206 (1965).
[10] M. H. Jericho, Phil. Trans. Roy. Soc. London **A257**, 385 (1965).
[11] R. E. Jones and A. M. Toxen, Phys. Rev. **120**, 1167 (1960).
[12] A. M. Toxen, G. K. Chang, and R. E. Jones, Phys. Rev. **126**, 919 (1962).
[13] C. B. Satterthwaite, Cambridge Superconductivity Conference, 1959 (unpublished).
[14] J. Bardeen, L. N. Cooper, and J. R. Schrieffer, Phys. Rev. **108**, 1175 (1955).
[15] L. P. Kadanoff and P. C. Martin, Phys. Rev. **124**, 670 (1961).
[16] J. Bardeen, G. Rickayzen, and L. Tewordt, Phys. Rev. **113**, 982 (1959).
[17] D. Markowitz and L. P. Kadanoff, Phys. Rev. **131**, 563 (1963).
[18] F. G. Brickwedde, H. van Dijh, M. Durleux, J. R. Clement, and J. K. Logan, J. Res. Natl. Bur. Std. (U. S.) **64A**, 1 (1960).

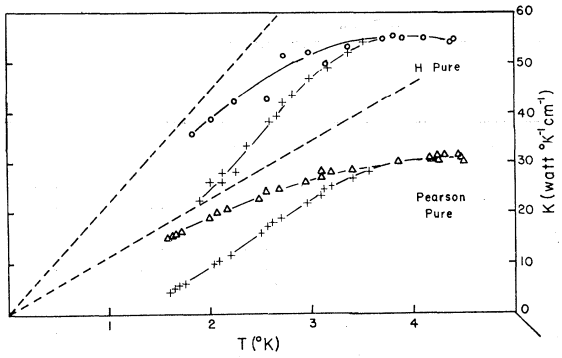

FIG. 1. Total normal- and superconducting-state thermal conductivities K^n and K^s versus temperature T, for Hulm's pure sample and the pure sample of this work. (○)—K^n for Hulm's pure, (△)—K^n for sample Sn1, this work. (+)—K^s for each sample. Dashed line—Wiedemann-Franz law.

The length between thermometers was determined with vernier calipers, and the sample diameters were measured with a traveling microscope. The uncertainties in these two quantities resulted in an A/L error of $\pm 1\%$. A correction for heat loss down the electrical leads from the hot end of the specimen was made and typically amounted to several percent of the total heat input. A much smaller correction was made for joule heating in the electrical leads to the heater. Radiation and gas conduction losses were negligible.

It was found necessary to make magnetic corrections on the normal-state conductivity for only two samples, Sn1 and Pb1. Following Hulm[2] and employing a formula due to Sondheimer and Wilson,[19] a correction was determined by measuring the thermal conductivity as a function of magnetic field at several temperatures above the transition temperature. The correction ranged from $2\frac{1}{2}\%$ at 1.5°K to 4% at 4.2°K for Pb1 and from 9% to 14% for Sn1.

For most samples, the scatter of the conductivity from a smooth curve drawn through the data was less than 1% (see Figs. 1, 2, 3, and 4). The worst case was that of the pure sample Sn1, which exhibited a scatter of $2\frac{1}{2}\%$. Geometrical uncertainties contribute to make the absolute magnitude of the conductivity somewhat more uncertain in each case, but fortunately these type of errors cancel in the ratio of the superconducting- to normal-state conductivities, K^s/K^n.

The technique used to determine the superconducting transition temperature T_c was similar to that described by Reynolds, Serin, and Nesbitt.[20] In independent runs on the same sample T_c was found to be reproducible

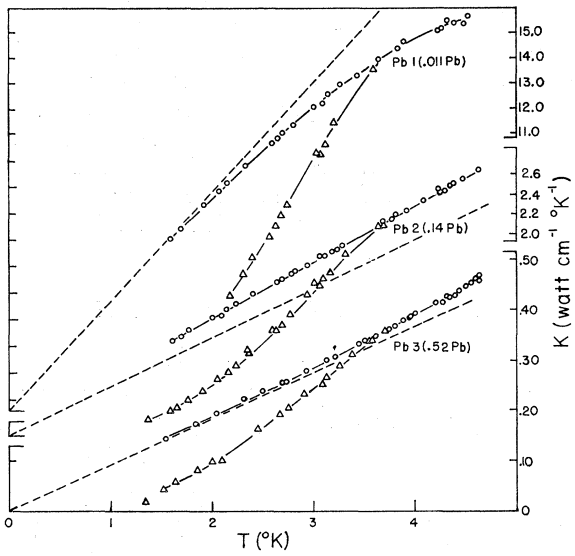

FIG. 2. Total normal- and superconducting-state thermal conductivities K^n and K^s versus temperature T, for the samples with lead impurity: Pb1, Pb2, and Pb3. Lead concentrations are given in atomic percent in parentheses. (○)—K^n, (△)—K^s, dashed line—Wiedemann-Franz law.

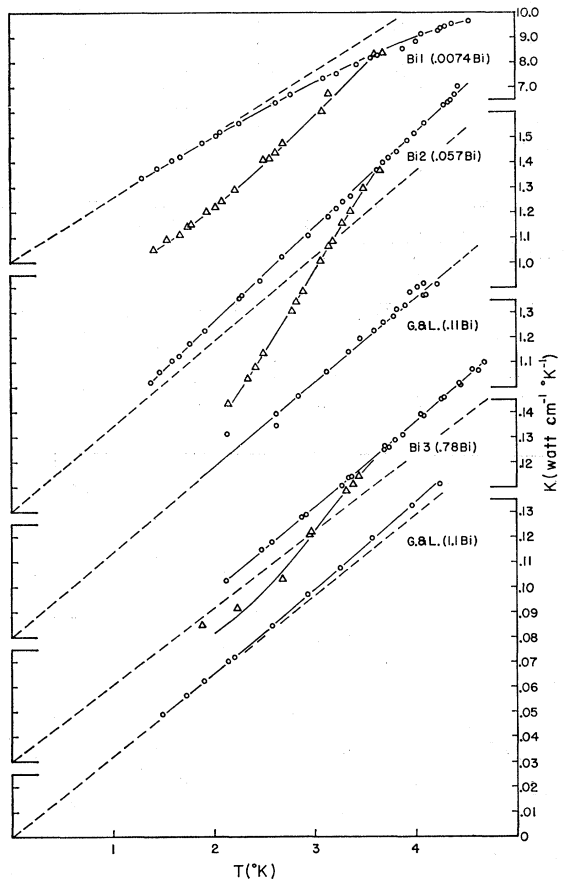

FIG. 3. Total normal- and superconducting-state thermal conductivities K^n and K^s versus temperature T, for the samples with bismuth impurity: Bi1, Bi2, and Bi3. Also shown are two samples of Garfinkel and Lindenfeld, G&L (0.11 Bi) and G&L (1.1 Bi). Bismuth concentrations are given in atomic percent in parentheses.

[19] E. H. Sondheimer and A. H. Wilson, Proc. Roy. Soc. (London) **A190**, 435 (1947).

[20] C. A. Reynolds, B. Serin, and L. B. Nesbitt, Phys. Rev. **84**, 691 (1951).

TABLE I. Experimentally determined quantities associated with several specimens of pure and impure tin.

Worker	Sample	At. % & Imp. type[a]	At. %[b]	$\rho_{4.2}$[c] ($\mu\Omega$ cm)	ρ_{273} ($\mu\Omega$ cm)	ρ_r	T_c	$\alpha\times10^4$	β	a
Present	Sn1	Pure	...	0.00213	13.06	0.0_3163	3.720	5.34	0.0976	0.282
Present	Pb1	0.011 Pb	0.011	0.00564	12.71	0.0_3444	3.716	6.98	0.228	0.120
Present	Pb2	0.10 Pb	0.14	0.0500	13.19	0.00381	3.713	...	...	...
Present	Pb3	0.98 Pb	0.52	0.00478	13.55	0.0_3382	3.752	...	...	...
Present	Bi1	0.007 Bi	0.0074	0.00578	12.61	0.0_3458	3.725	8.6	0.395	0.070
Present	Bi2	0.08 Bi	0.057	0.0721	11.91	0.00609	3.709	...	...	...
Present	Bi3	0.88 Bi	0.78	0.796	13.31	0.0636	3.700	...	...	...
Present	Hg1	0.011 Hg	0.011	0.0203	12.87	0.00158	3.718	10.1	0.71	0.039
Present	Hg2	0.10 Hg	0.031	0.113	11.28	0.0101	3.686	...	...	...
Present	Hg3	1.1 Hg	0.23	0.475	13.35	0.0543	3.646	...	...	...
Hulm	...	Pure	...	0.0011	...	...	3.71	3.92	0.048	0.42
Hulm	...	0.033 Hg	...	0.0141	...	...	3.68	5.70	0.656	...
Hulm	...	0.33 Hg	...	0.165	...	...	3.72	...	...	...
G & L	...	0.11 Bi	...	0.0721	...	...	...	...	...	...
G & L	...	1.1 Bi	...	0.758	...	...	...	...	...	...

[a] Calculated from amount of impurity added to melt.
[b] Results of Jarrell-Ash spectroscopic analysis.
[c] These values are referred to in the text as ρ_0.

to within ±0.004°K. This, the largest error, was small enough to permit a comparison of the data to the results of Lynton *et al.*[21] relating impurity concentration to change in T_c, and the agreement was quite satisfactory.

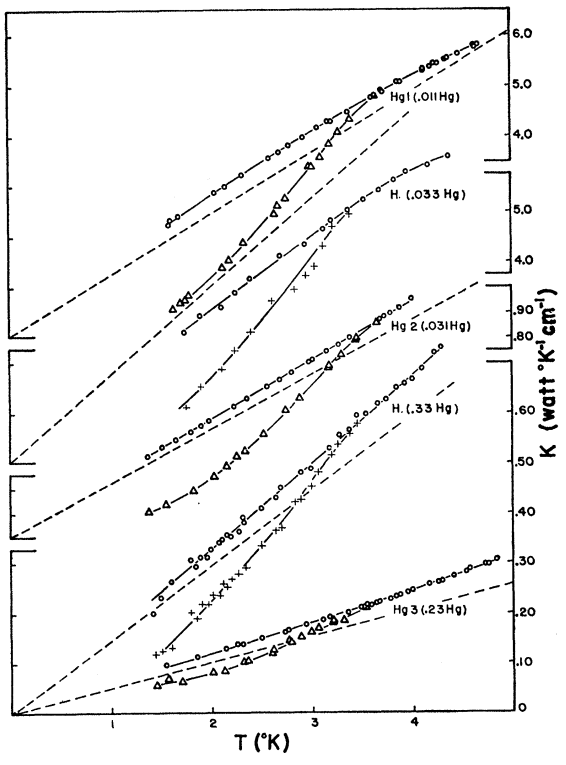

FIG. 4. Total normal- and superconducting-state thermal conductivities K^n and K^s versus temperature T, for the samples with mercury impurity: Hg1, Hg2, and Hg3. Also shown are two samples of Hulm, H.(0.033 Hg) and H.(0.33). Mercury concentrations are given in atomic percent in parentheses.

[21] E. A. Lynton, B. Serin, and M. Zucker, J. Phys. Chem. Solids **3**, 165 (1957).

(However, for more information concerning change in T_c, see a later work of ours, Ref. 22.)

Electrical-resistance measurements were subsequently made at 273 and 4.2°K on ~5-cm lengths of the samples cut from between the resistance thermometers. The conventional four-probe method was employed, using a Leeds and Northrup K-2 potentiometer. Length and diameter measurements were made with a traveling microscope. Geometrical errors and uncertainties in the resistance determinations led to experimental uncertainties in ρ_{273} and ρ_0 of 0.7 and 1.5%, respectively. In Table I we list the quantities associated with each of our specimens as well as some results by other investigators which are pertinent to the discussion to follow. $\rho_r=\rho_0/(\rho_{273}-\rho_0)$ is the usual residual resistivity ratio. The values of $d\rho_r/dx$ inferred from the data in Table I are 0.04, 0.08_5, and 0.15_5 per at. % for Pb, Bi, and Hg impurity, respectively. We note that the low ρ_0 value for Pb3 is anomalous. This presumably is caused by the occurrence of a lead-enriched phase along the grain boundaries in this specimen which could be superconducting at 4.2°K.

III. RESULTS AND DISCUSSION

A. Thermal Conductivity

Figures 1, 2, 3, and 4 exhibit the thermal-conductivity data, both those of the normal and of the superconducting states, of the present specimens. The data of other investigators taken on samples with comparable impurity concentrations and identical impurity type are also shown for purposes of comparison. The straight dashed line associated with each set of data is the line the normal-state data would fall on if the Wiedemann-Franz Law were perfectly obeyed. We note that the

[22] J. E. Gueths, C. A. Reynolds, and M. A. Mitchell, Phys. Rev. **150**, 346 (1966).

impurity concentrations in Fig. 4 appear to be out of order when compared against Hulm's impurity concentrations. This is not unreasonable, as his impurity concentration is that added to the melt from which the specimen was prepared. Inspection of Table I reveals that the amount of Hg added to the melt in our case was significantly larger than the value obtained from spectroscopic analysis.

At intermediate impurity concentrations, the normal-state thermal-conductivity data is very nearly linear in T, suggesting that the normal-state lattice conductivity is negligible, and that the electronic thermal resistivity is dominated by electron-impurity scattering. However, the slope of the K^n-versus-T line differs from L_0/ρ_0 in most cases by several percent. It is not clear what causes this deviation, but errors in geometrical determinations could be a contributing factor. The Wiedemann-Franz line associated with Pb3 was constructed artificially since, as previously discussed, the $\rho_{4.2}$ measurement was anomalous.

Since the specimens with 0.1–1.0% impurity exhibit a normal-state thermal conductivity nearly linear in T, it is clear that a meaningful separation into electronic and lattice components by conventional means[23] would be extremely difficult, as the difference of two very large quantities would be involved. However, the superconducting-state lattice conductivity K_g^s forms a much larger fractional part of K^s, and we can obtain some information about K_g^n by employing a more unconventional technique.

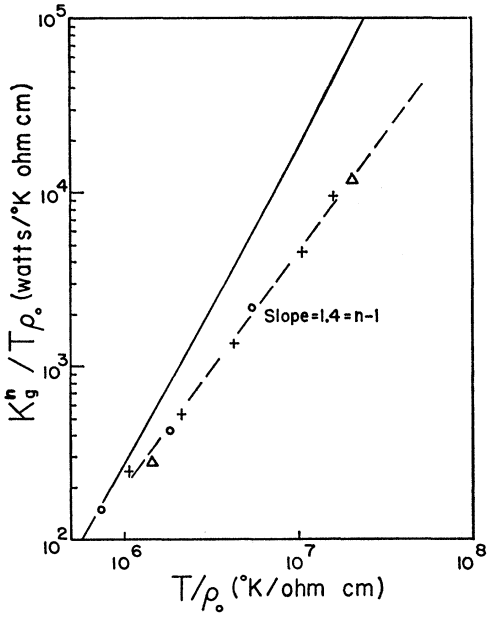

FIG. 5. The universal curve of Lindenfeld and Pennebaker scaled to tin. The solid curve is the theoretical curve for the case in which the longitudinal and transverse modes are independent and the total lattice conductivity is a simple sum. The ○'s, +'s, and △'s are representative points taken from the curves for silver, copper, and indium and scaled to a tin curve. The dashed line is drawn through these points and has a slope of $n-1$, where n is the exponent of the temperature dependence of K_g^n [see Eq. (6)].

As mentioned in the introduction, Lindenfeld and Pennebaker[8] have applied Pippard's theory of ultrasonic attenuation to a theory of the normal-state lattice conductivity with a reasonable degree of success. Their experimental results on copper as well as those of Jericho on silver[10] and Lindenfeld and Rohrer on indium[9] strongly suggest that a "universal" function relating $K_g^n/T\rho_0$ to T/ρ_0 exists for dilute alloy systems when the scattering of phonons by electrons dominates the lattice thermal resistivity in the normal state. In Fig. 5 we show such a plot scaled for tin. The extended solid line represents a theoretical K_g^n relationship for the case when the transverse and longitudinal modes operate independently and their respective conduction processes can be added. The data in Fig. 5 are representative points taken from curves relating $K_g^n/T\rho_0$ to T/ρ_0 for copper, silver, and indium which have been scaled to a tin curve in the manner suggested by Lindenfeld and Pennebaker. It is seen that the suggestion of a universal function is experimentally substantiated, as all of the scaled data seem to lie on the same curve. Even though there appears to be some disagreement between the absolute value of theory and experiment on this plot in the region of long electronic mean free paths, the data for the various host metals are at least consistent in this respect. Possible reasons for this apparent disagreement between theory and experiment have been discussed previously.[8,9,24]

Figure 5 suggests that we should expect to find $K_g^n = CT^n$ where $n=2.4$. Furthermore, if indeed the magnitude of K_g^n is roughly given by the dashed line in Fig. 5 as a function of ρ_0 and T, K_g^n will be a fractionally small part of K^n, amounting to only ~4% of K^n at $T=4$°K for our most impure specimen. This is consistent with our earlier observation that, because of the linear variation of the K^n-versus-T curves, the lattice conductivity did not form a large part of K^n for any of our specimens. However, we use the variation of the ratio K^s/K^n with ρ_0 to obtain some information about K_g^n in these specimens.

In Fig. 6 we show the ratio K^s/K^n for the more impure specimens measured in this work. The upward trend of K^s/K^n for the most impure specimens as $t = T/T_c$ is reduced is presumably a manifestation of K_g^s, which forms a large part of K^s at these low temperatures. The calculations of Klemens and Tewordt[25] indicate that the BRT ratio

$$R_g = K_g^s/K_g^n \tag{5}$$

has a ρ_0 dependence, but in the dilute impurity range

[23] P. G. Klemens, in *Encyclopedia of Physics*, edited by S. Flügge (Springer-Verlag, Berlin, 1956), Vol. 14, p. 260.

[24] C. Feldman, Phys. Rev. **139**, A211 (1965).

[25] P. G. Klemens and L. Tewordt, Rev. Mod. Phys. **36**, 118 (1964).

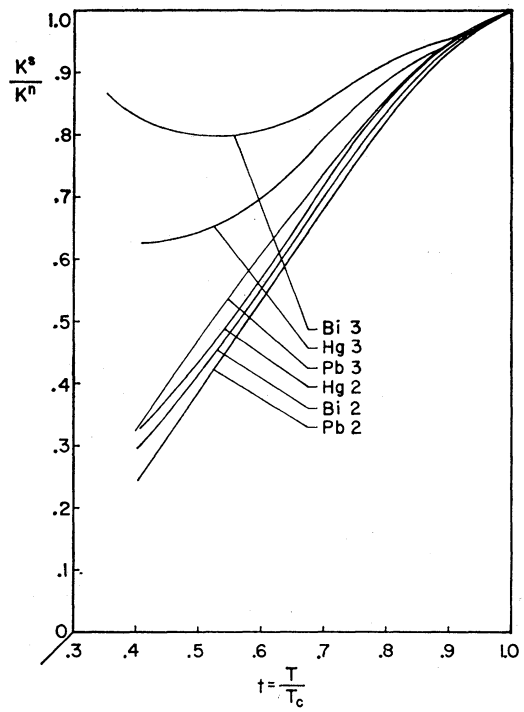

FIG. 6. The ratio of the total thermal conductivities K^s/K^n versus reduced temperature $t=T/T_c$, for the six higher impurity samples.

of this work this variation is expected to be so slight that we will ignore it.

As suggested by Fig. 5, we assume that an approximate relationship between $K_g{}^n$, T, and ρ_0 exists in the very dilute range of the form

$$\ln(K_g{}^n/T\rho_0)=A+(n-1)\ln(T/\rho_0), \tag{6}$$

where n is the temperature dependence of $K_g{}^n$. Thus, combining Eqs. (5) and (6), we have

$$\ln(K_g{}^s/T\rho_0 R_g(t))=A+(n-1)\ln(T/\rho_0). \tag{7}$$

A fractionally large normal-state lattice conductivity is not apparent in any of the data in Figs. 1, 2, 3, and 4. In fact, from Fig. 5, we expect that $K_g{}^n/K^n\leq 0.03$ for all of our specimens, so that, to a very good approximation,

$$K^s/K^n=K_e{}^s/K_e{}^n+K_g{}^s/K_e{}^n. \tag{8}$$

The results of Guenault[1] show that the ratio $K_e{}^s/K_e{}^n$ is strongly influenced by (a) the crystal orientation, and (b) the ratio of the electron-phonon scattering to electron-impurity scattering. The influence of (b) should not be seen here, as the values of ρ_0 and T which concern us make this ratio small for all samples. Thus for specimens having the same crystal orientation, we expect that

$$(K^s/K^n)=(K^s/K^n)_{\rho_0\to 0}+K_g{}^s/K_e{}^n, \tag{9}$$

where $\rho_0\to 0$ means the limiting value of K^s/K^n as the impurity is reduced to zero and the influence of the electron-phonon scattering is neglected. Figure 7 demonstrates this well at $t=0.75$. The data of Guenault demonstrate the effects of the anisotropy of $K_e{}^s/K_e{}^n$ for nearly pure specimens. Hulm's samples were cast and consisted of several large crystals, and thus are expected to have the tetrad axis nearly perpendicular to the specimen axis. Comparison of his data to the data of Guenault for the perpendicular direction would indicate that this is the case. The present specimens were extruded wire and the orientation was in question. The ρ_{273} values listed in Table I would indicate that they should be considered to be more nearly parallel, if the anisotropic electrical resistivity[26] is indeed a measure of an average orientation of the small crystals which make up the specimens. One can see that in the limit of decreasing ρ_0, they indeed appear to be more parallel if judged against Guenault's results in Fig. 7. If we conditionally assume that all of the present specimens have essentially the same orientation, the line drawn through the present data in Fig. 7 yields an estimate of $(K^s/K^n)_{\rho_0\to 0}$.

Combining Eqs. (7) and (9), and using the Wiedemann-Franz relation $K_e{}^n=TL_0/\rho_0$, we see that

$$\ln\left[\frac{K^s}{K^n}-\left(\frac{K^s}{K^n}\right)_{\rho_0\to 0}\right]=\ln\frac{R_g C T^{n-1}}{L_0}+(3-n)\ln\rho_0. \tag{10}$$

At constant t,[27] Eq. (10) describes a straight line, exponent of the temperature dependence of $K_g{}^n$ being n. Figure 8 shows several plots of the type described by Eq. (10) at $t=0.45$, 0.60, and 0.75. The slopes $(3-n)$ of the three lines are 0.70, 0.68, and 0.63, respectively. Thus, Eq. (10) seems to be roughly satisfied, with n approximately independent of T. The points at low ρ_0

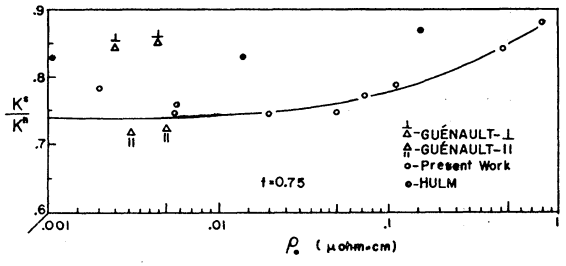

FIG. 7. The ratio of the total thermal conductivities K^s/K^n versus residual electrical resistivity ρ_0 at $t=0.75$. (○), the experimental points of this work. (●), experimental points of Hulm. △, experimental points of Guenault: marked ⊥ for the case when the c axis was perpendicular to the specimen axis and hence to direction of current or heat flow; marked ∥ for the case when the c axis was parallel to the specimen axis. The solid curve is drawn through the data in order to obtain $(K^s/K^n)_{\rho_0\to 0}$.

[26] J. E. Gueths, M. A. Mitchell, and C. A. Reynolds, Bull. Am. Phys. Soc. **11**, 74 (1966).

[27] The variation of T_c with composition is too small to affect this equation to any significant degree.

are especially susceptible to small errors in $(K^s/K^n)_{\rho_0\to 0}$ and orientation effects. Thus the lines have been drawn with the greatest emphasis on the highest ρ_0 data. The effects of the αT^2 scattering term in $K_e{}^n$ are not yet apparent in Figs. 7 or 8. At even lower values of ρ_0 than those considered here, this term tends systematically to decrease the ratio K^s/K^n until electron-phonon scattering is the only source of electronic thermal resistivity. Since the error in each of these curves is relatively large, we take an average value of n to be 2.35. The dashed line in Fig. 5 is a line exhibiting a temperature dependence of $K_g{}^n$ of this value.

Using this temperature dependence for $K_g{}^n$, we have analyzed the three most impure specimens by drawing the best line through the normal-state data of the form suggested by the analysis up to this point,

$$K^n/T=1/\beta+DT^{1.35}. \tag{11}$$

The results of this analysis, as well as those of some previous investigations on tin, are shown in Fig. 9. Shown also are the solid and dashed lines which were introduced in Fig. 5. The agreement between the data

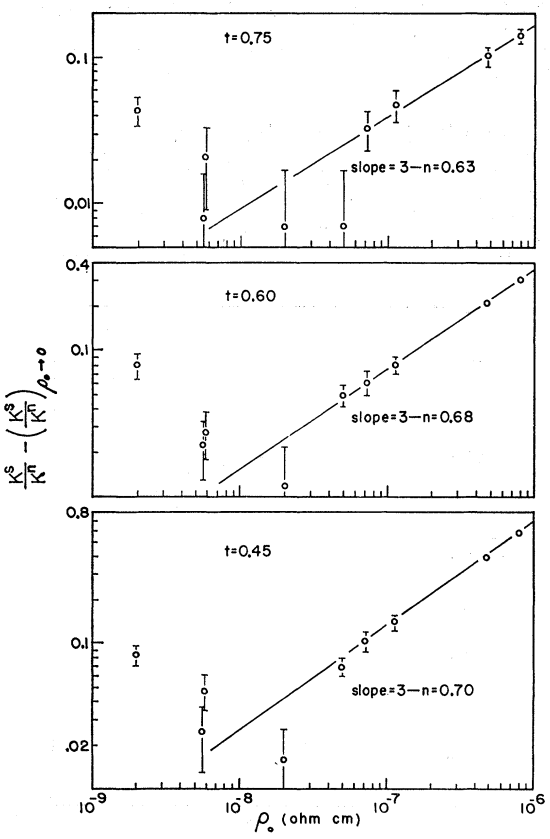

FIG. 8. Plots of the difference between the ratio of the total thermal conductivities K^s/K^n and $(K^s/K^n)_{\rho_0\to 0}$ versus residual electrical resistivity ρ_0 at three values of reduced temperature. Estimated uncertainties due to scatter in K^s and K^n are indicated by the error bars. The slopes of the solid lines are taken to be $(3-n)$, where n is the exponent of the temperature dependence of $K_g{}^n$ [see Eq. (10)].

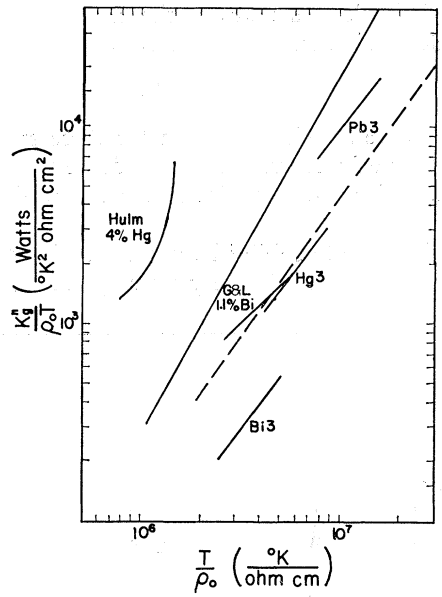

FIG. 9. Comparison of the normal-state lattice conductivities of tin with the universal curve. The extended solid and dashed lines are the "theoretical" lines of Fig. 5. Individual data points have been omitted to avoid confusion. That the present results are parallel to the dashed line is perhaps fortuitous, as the slope is, to a degree, preselected by the type of analysis described in the text. The results obtained by Garfinkel and Lindenfeld and Hulm on their specimens in this region of ρ_0 are also shown.

and the quasitheoretical (dashed) line of Fig. 9 leaves much to be desired, but order of magnitude agreement is certainly realized.

From Eq. (10) and curves of the type in Fig. 8, we also expect to obtain information about R_gC as a function of t. In particular, if we assume that C is given by the "universal" (dashed) line of Fig. 5 ($C=2\times 10^{-6}$), we can obtain $R_g(t)$. In Fig. 10, we have plotted values of R_g obtained in this manner at five reduced temperatures. It is seen that they compare favorably with the BRT prediction.

To summarize, we see that a complete separation of the normal and superstate data into electronic and lattice contributions has not been realized, due to the small size of $K_g{}^n/K^n$ and possibly large orientation effects. However, the data certainly appear to be consistent with data on other alloy systems and with the concept of a universal curve relating $K_g{}^n$ to ρ_0 and T. Furthermore, upon using the theoretical Lorenz number and a constant obtained from the universal curve, the ratio $K_g{}^s/K_g{}^n$ is in good agreement with the BRT predictions.

B. The Superconducting Energy Gap

We now expect that $K_g{}^n$ and $K_g{}^s$ should become fractionally smaller portions of the total conductivities as ρ_0 decreases. The normal-state data of the four lowest impurity samples Sn1, Pb1, Bi1, and Hg1 were conse-

quently fit by least squares to the conventional form for the electronic thermal conductivity

$$T/K_e^n=\alpha T^3+\beta. \quad (12)$$

In Fig. 11, we see that the data for these specimens satisfactorily exhibit the linear dependence of Eq. (12). The values of α and β obtained from this analysis are listed in Table I.

Other investigators[1,5,11,13] have compared the variation of K^s/K^n with t for very pure specimens to the

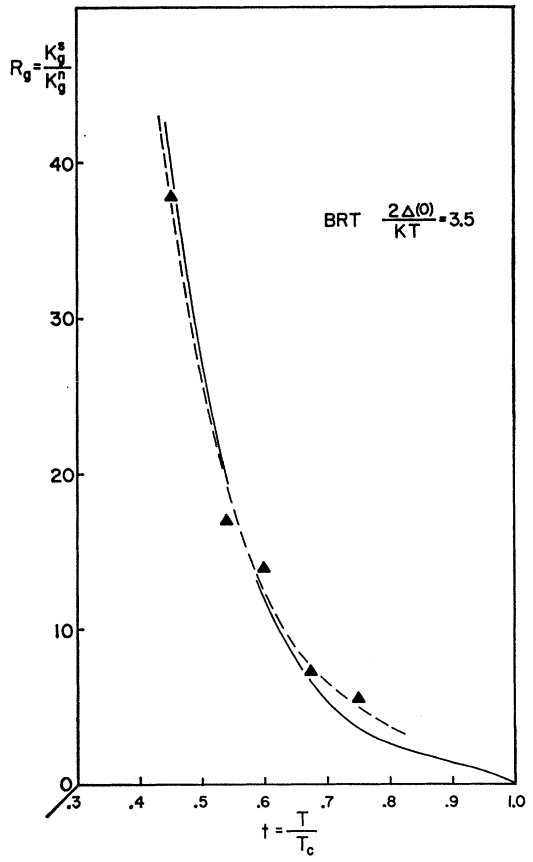

FIG. 10. The ratio of the lattice conductivities K_g^s/K_g^n versus reduced temperature. The solid curve is the theoretical one of BRT for $2\Delta(0)/k_BT_c=3.5$. (▲)—the points calculated from the data of this work as indicated in the text. The dashed curve is a curve through these points.

theoretical predictions of Kadanoff and Martin with a reasonable degree of success. Theoretically, the ratio of the electronic parts of the thermal conductivity, K_e^s/K_e^n, is given by an integral[15] involving two parameters: $2\Delta(0)/k_BT_c$, where $\Delta(0)$ is the energy gap for the formation of quasiparticle excitations at absolute zero, and a, the ratio of the electronic thermal resistivity due to phonon scattering to that due to impurity scattering evaluated at the critical temperature. a can be expressed in terms of the normal-state parameters in Eq. (12) as $a=(\alpha/\beta)T_c^3$. Of course, as the

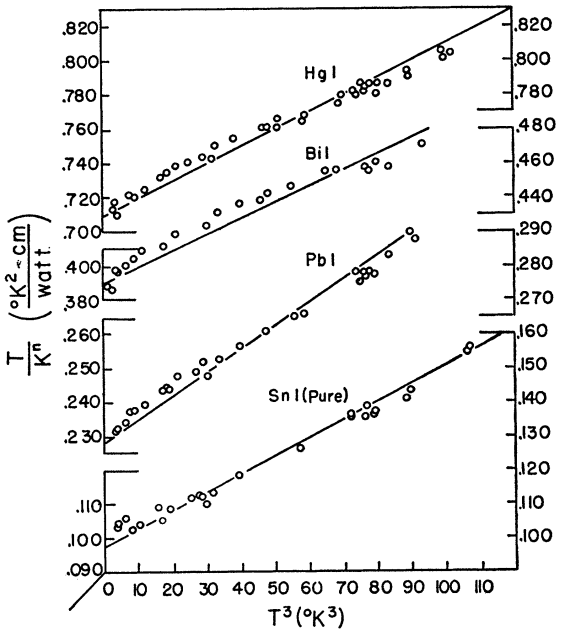

FIG. 11. T/K_e^n versus T^3. A test of Eq. (12) for the four low-impurity samples. The fact that K^n can be used instead of K_e^n indicates that the conductivity is essentially electronic. The straight lines are least-squares fits to the experimental data.

sample purity increases, a increases. The values of a for the four least impure specimens are listed in Table I.

In Fig. 12 the data for Sn1 is compared to the theoretical curve with $a=0.5$ and $(2\Delta(0)/k_BT_c)=3.3$. Comparison to the theory for Pb1, Bi1, and Hg1 is made in

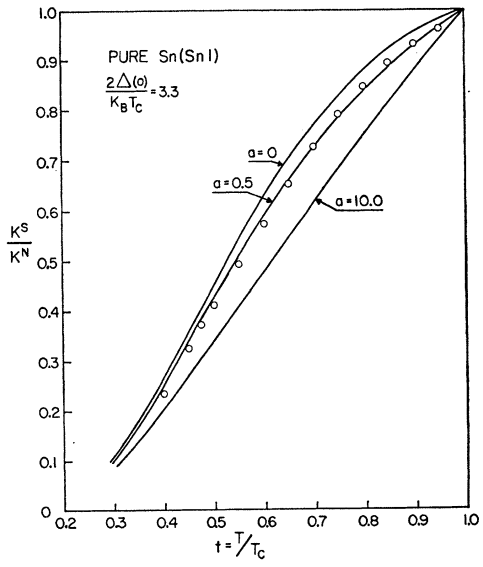

FIG. 12. A plot of total thermal conductivity K^s/K^n versus reduced temperature. (○)—the experimental values for the pure sample Sn1. The solid curves are plots of the Kadanoff and Martin theoretical values of K_e^s/K_e^n for an energy-gap parameter $2\Delta(0)/k_BT_c=3.3$ and for three values of $a=(\alpha/\beta)T_c^3$, $\alpha=0$, 0.5, and 10.

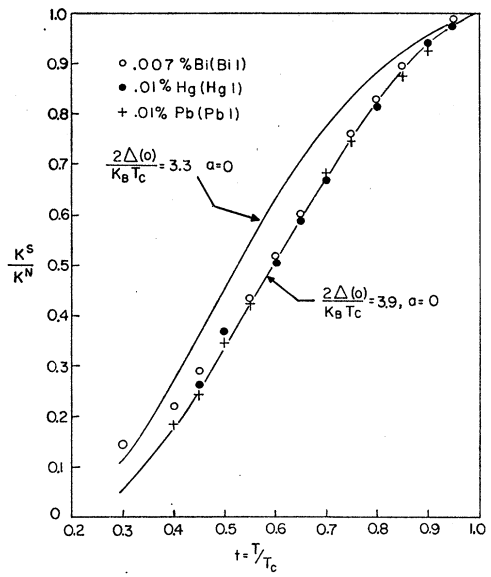

FIG. 13. A plot of the total thermal conductivity ratios K^s/K^n versus reduced temperature. (+, ○, ●) experimental values for the three 0.01% (nominal) specimens Pb1, Bi1, and Hg1. The upper solid curve is the Kadanoff and Martin theoretical calculation of K_e^s/K_e^n for an energy-gap parameter $2\Delta(0)/k_BT_c=3.3$ and $a=(\alpha/\beta)T_c^3=0$. The bottom curve is that for an energy-gap parameter of 3.9 and $a=0$.

Fig. 13 with $a=0$ and $(2\Delta(0)/k_BT_c)=3.9$. The surprising aspects of these data are that the energy gap had to be increased to 3.9 to fit the theoretical curve to the data, and that a single theoretical curve passes through all of the 0.01% data over most of the temperature range. The latter point seems to indicate that whatever causes the apparent change in the energy gap is independent of the kind of impurity present in the metal.

We cannot attribute this shift to the presence of significant fractions of either K_g^n or K_g^s in these specimens. Besides having no evidence for lattice conductivities in these specimens, we would expect to find a shift in the opposite sense if the lattice conduction were a fractionally larger portion of the total for the 0.01% samples than in the pure specimen. Also we cannot reasonably attribute this shift to a change in net crystal orientation. An examination of ρ_{273} values in Table I and a comparison of these values with measurements of ρ_{273} versus crystal direction[26] indicate that there is no significant change in net orientation between the pure and the nominal 0.01 at. % samples.

One might be led to conclude that the isotropic BCS-type energy gap that is assumed in this comparison depends on impurity concentration. However, Anderson[28] proved that an isotropic gap is unaffected by impurities. Further, he showed that for the case of an anisotropic gap, the primary effect of impurities is to smooth out the anisotropy. Since then several experiments, notably on optical absorption[29] and on ultrasonic absorption,[30] have demonstrated directly the smoothing of gap anisotropy by impurities. The data reported in the present paper indicate that thermal conductivity is also incapable of explanation on the basis of an effective isotropic gap, but rather requires a full investigation of energy-gap anisotropy and its reduction by impurities. Such an investigation is carried out in the paper following by Ulbrich *et al.*[31]

ACKNOWLEDGMENTS

The authors wish to acknowledge helpful discussions with Professor R. H. Bartram, Professor P. Lindenfeld, Professor D. Markowitz, and Professor A. H. Spees, and technical assistance by H. Taylor and A. Newman. The computational part of this work was carried out in the Computer Center at the University of Connecticut, which is supported in part by grant GP-1819 of the National Science Foundation.

[28] P. W. Anderson, J. Phys. Chem. Solids **11**, 26 (1959).
[29] P. L. Richards, Phys. Rev. Letters **7**, 412 (1961); J. D. Leslie and D. M. Ginsberg, Phys. Rev. **133**, A362 (1964).
[30] L. T. Claiborne and N. G. Einspruch, Phys. Rev. Letters **15**, 862 (1965).
[31] C. W. Ulbrich, D. Markowitz, R. H. Bartram, and C. A. Reynolds, following paper, Phys. Rev. **154**, 338 (1967).